INFORMATION CONSTRAINED CONTROL FOR VISUAL DETECTION OF IMPORTANT AREAS

Ron M Hecht [1,3], Ariel Telpaz[1], Gila Kamhi[1], Aharon Bar Hillel[2], Naftali Tishby [3]

[1]*GM-R&D ATC-Israel UXT*
[2]*Dept. of Industrial Engineering and Management, Ben-Gurion University, Israel*
[3] *School of Engineering and Computer Science, Hebrew University, Israel*

ABSTRACT

In this work, we propose a method for detection of locations with subjective significance in the visual environment using Information Constrained Control (ICC). ICC is a model that takes into consideration not only the goal but also the complexity of the control needed to achieve it, characterized by its deviation from default behavior. This concept resonates with the human visual attention system, which includes an interaction between top-down goal oriented pressure and bottom-up processes of common gaze behavior. We start by providing rationale and intuition for ICC based analysis, then formalize it. Specifically, we formalize a mechanism for estimation of subjective significance. Later, we theoretically compare the ICC to the commonly used STD based mechanism, present the latter as a special case of ICC, suggesting an ICC reward visualization mechanism for STD. Finally, we describe our experiment in a real-world driving environment and present empirical finding to support our claim.

Index Terms—Information Constrained Control, Eye gazes, Workload.

1. INTRODUCTION

Our visual system does not observe the entire field of view with the same cone density. The center part of the field of view is observed by the Fovea, that has much higher density relative to the rest of the visual system. Having one part of the visual system with higher density, requires the visual system to allocate it wisely. This allocation in the human visual system occurs by an entanglement of top-down and bottom-up processes [1]. Top-down process refers to movement of the Fovea towards task related locations in the Visual Environment (VE). By bottom-up we refer to exploration like behavior i.e. movement of the Fovea towards general salient area in the field of view [2], where 'saliency' here is non-goal driven criterion.

Overall, there are two contradicting goals. On one hand, the visual system would like to explore its surrounding as much as possible; however, on the other hand, it would like to focus on its current task. This dual goal situation is solved by selecting a tradeoff between the two. In her work [1], Lavie suggested that the tradeoff is influenced by workload. At high workload, the system focuses on the task at hand and presents a top-down behavior. At low workload, it drifts away towards salient regions as the bottom-up approach suggests. Lavie described this phenomena by observing the ability to pay attention to objects outside the fovea field of view. The change in eye gaze distribution across the VE as function of the workload, was explored at [3]. More specifically, they suggest that the Standard Deviation (STD) of the distribution gets narrower as the workload increases. Other related work regarding saliency and attention [4] [5] [6] [7] [8] [9].

In this work, the change in eye gaze is explained using the Information Constrained Control (ICC) [10] [11] [12] [13] [14]. At first, we provide a diagram level explanation to the behavior. Later, we derived the specific equations. Finally, we show that the STD approach [3] can be presented as a specific case of ICC. Ultimately, we show empirical finding that support ICC like behavior.

2. BLOCK DIAGRAM BEHAVIOR

We present a high-level block diagram of ICC in Figure 1 to help develop intuition and insights, with full formalization deferred to later sections. Let's assume a system that at any given time estimates two distributions over the VE: distribution of the salient locations in the VE, and distribution of the important locations (from task perspective) in the VE. The distributions are estimated by the "Saliency distribution estimator", and the "Important location distribution estimator" respectively. At the next step, the system uses the "Saliency based sample generator" to generate a long sample of locations for the Fovea to look at. This sample is drawn from the saliency distribution. Once the sample is generated, it transmitted for evaluation by the "Important location evaluator". The evaluator compares the sample to the distribution of task important locations. The system desires that the overlap between the sample and the distribution will be high enough. In case that the sample is not satisfactory, a resample message is send and new sample is drawn. This iteration is repeated till a good enough sample is achieved. This sample is ultimately transmitted for execution.

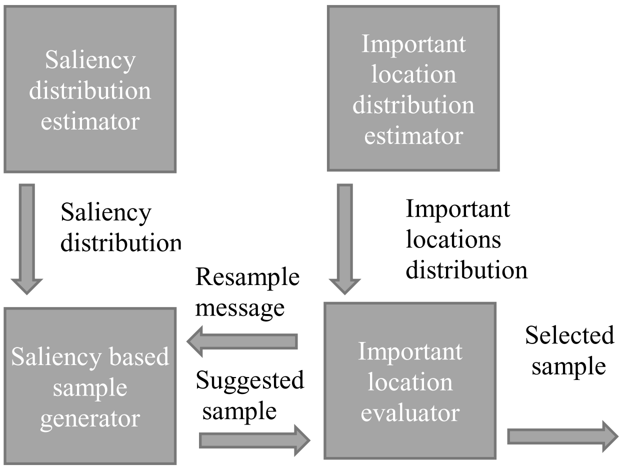

Figure 1. Block diagram

Intuition can be gained as well by imagining a lazy system. A system that achieves its goal while selecting a behavior that is as close as possible to its comfort zone behavior. A system that does not desire to excel, just to be good enough. We do not claim that this system is implement in the human visual system.

3. INFORMATION CONSTRAINED CONTROL FORMALIZATION

The ICC is formalized as minimization subject to constrains. The n objects in VE are denoted as $\alpha_1, \dots, \alpha_n$. Each object is represented by two values: $Q(\alpha_i)$ its saliency value and $R(\alpha_i)$ its importance to the task. More specifically, we formalize the importance as reward, the reward that is gained when focusing on object α_i.

The goal of the two upper blocks presented in Figure 1 ("Saliency distribution estimator" and "Important location distribution estimator") is to estimate those two values: R and Q. They provide the entire R and Q distributions for all the objects, as the arrows downwards in the figure suggests.

The block "Saliency based sample generator" draws a sequence of actions $A = a_1, \dots, a_T \quad a_t \in \{\alpha_1, \dots, \alpha_n\}$ according to the distribution Q. We denote the distribution of the drawn sequence by P_A where:

$$P_A(\alpha_i) = 1/T \sum_{t=1}^{T} \delta(a_t = \alpha_i) \tag{1}$$

Later, the sequence A is sent to the "Important location evaluator" block. This block evaluates V_A the average reward according to the distribution R:

$$V_A = 1/T \sum_{t=1}^{T} R(a_t) = \sum_{i=1}^{N} R(\alpha_i) P_A(\alpha_i) \tag{2}$$

The goal of the block "Important location evaluator" is to forward the sequence A only if its value V_A is above or equal to a threshold θ. In cases where $V_A < \theta$, the block asks for a new sequence to be drawn. Large Deviation Theory and specifically Sanov Theorem [15] suggests that in such cases the selected sequence will satisfy the following inference problem:

$$P_A(\alpha_i) = \underset{\substack{P \\ s.t \\ \sum_{i=1}^{N} R(\alpha_i) P(\alpha_i) = \theta \\ \sum_{i=1}^{N} P(\alpha_i) = 1}}{\arg\min} \sum_{i=1}^{N} P(\alpha_i) \ln \frac{P(\alpha_i)}{Q(\alpha_i)} \tag{3}$$

This equation presents the duality of the goal. On one hand the minimization of the distance between P_A and Q where the distance is measured using the Kullback Leibler divergence (D_{KL}) [15]. On the other hand, there is a strict need to achieve a needed level of average reward θ.

The equation can be minimized subject to the constraints by using Lagrange multipliers. The solution is that case has the following form:

$$P_A(\alpha_i) = \frac{1}{Z(\theta, \beta)} Q(\alpha_i) e^{\beta(\theta) R(\alpha_i)} \tag{4}$$

where β is the Lagrange multiplier and is a function of θ. Z is the normalization factor.

4. EXTRACTION OF THE REWARD DISTRIBUTION

The solution presented in Eq. 4 enables us to estimate P_A the expected distribution in cases where R and Q are known. In cases where only P_A and Q are available, R can be expressed as a linear equation of the log likelihood of P_A and Q:

$$\ln \frac{P_A(\alpha_i)}{Q(\alpha_i)} = \beta(\theta) R(\alpha_i) - \ln Z(\theta, \beta) \tag{5}$$

Unfortunately, in many cases, both R and Q are not known or observed. Let's consider such case where the only observed distributions are eye gaze distribution under two different levels of workload: relaxed workload condition and common one. We denote the associate gaze distributions for relaxed and common conditions as P_R and P_C respectively. In such case, the following equation shows that the log likelihood ratio of the two distributions P_R and P_C are a linear function of the reward.

$$\begin{aligned} \ln \frac{P_C(\alpha_i)}{P_R(\alpha_i)} &= \ln \frac{P_C(\alpha_i)}{Q(\alpha_i)} - \ln \frac{P_R(\alpha_i)}{Q(\alpha_i)} = \\ &= \big(\beta_C(\theta_C) - \beta_R(\theta_R)\big) R(\alpha_i) \\ &\quad - \ln Z(\theta_C, \beta_C) + \ln Z(\theta_R, \beta_R) \end{aligned} \tag{6}$$

The last equation is a useful tool and has deep implications to the analysis of tasks under varying workload conditions. By using this equation, one can visualize the reward associated with each object α_i in the field of view and identify the important ones. It is important to mention that until now, we did not have to define what an object is, or what type of distribution we are using. The distribution can be discrete or even parametric. In this work we define the objects to be discrete, "pixel" like location in the VE. More specifically we organize them in a 2D matrix associated with the x, y coordinate in the VE. As shown in the equation, we are estimating the reward up to a linear function. However, in cases where condition C is selected to be the higher workload, a monotonic positive relation exists between the estimated reward value and the real reward value. i.e. an object that has higher real reward value than another, has higher estimated reward value. Specifically, the object with the maximal real reward value, is the one with the highest estimated one. The same goes for the minimal value. In addition, let's recall that in many real-world cases the reward values are selected to maintain an order and their absolute values are less important. Our suggested approach is even more effective in such cases. Overall, we presented a mechanism for visualization. Given the relation between visualization and intuition, we provide a mechanism to better understand the task at hand.

5. ADDING REWARD VISUALIZTION CAPABILITIES COMPARISON STANDARD DEVIATION APPROACH

It is not clear whether the STD approach was suggested with visualization capabilities; however, here we provide it with such by defining it in ICC terms. We start by defining P_R and P_C. The STD does not provide claims regarding the distribution itself. It leaves too many possibilities regarding the manner in which the condition changes in the distribution. In order to have a well-defined distribution, we selected a parametric distribution whose only parameter is STD – 2D diagonal Gaussian with a fixed mean. Let's recall that such Gaussian is 1D Gaussian multiplied by another one. Therefore, we start by analyzing a 1D Gaussian, and later extend in to 2D.

5.1. Single Dimension

We assume that the distributions P_R and P_C are 1D Gaussians and Q is uniform distribution.

$$\ln P_{C,R}(\alpha) =$$
$$= -{}^{1}\!/_{2} \ln 2\pi - \ln \sigma_{C,R} - {}^{1}\!/_{2} \left(\frac{\alpha - \mu_{C,R}}{\sigma_{C,R}} \right)^2 \qquad (7)$$

The ratio $\ln \frac{P_C(\alpha)}{P_R(\alpha)}$ need to be linear, and that occur for any two Gaussians that share the same mean. The slope of the linear function is: σ_C^2 / σ_R^2.

5.2. Two Dimensions

Two-dimensional Gaussian distribution with diagonal covariance is actually two single dimensional Gaussians multiplied by one another $P(\alpha_x, \alpha_y) = P(\alpha_x)P(\alpha_y)$. So, in order to verify linearity all that we need to assure is:

$$\frac{\sigma_{Cx}^2}{\sigma_{Rx}^2} = \frac{\sigma_{Cy}^2}{\sigma_{Ry}^2} \qquad (8)$$

This equation shows that STD ratio is a specific case of ICC.

6. METHOD

We designed an experiment to test the reward visualization capabilities of the ICC. Inspired by Occam's razor, we designed the experiment to be the simplest one that can produce non-trivial results. We conducted an on-road experiment, conducted on real roads in real conditions. We chose such an environment since it is very immersive and real (not simulated). In addition, the participants are familiar with driving on a daily basis.

6.1. Participants

Fourteen participants (age: average = 46 standard deviation = 11) were recruited to participate in the study. Unfortunately, the GPS data was not collected properly for the first four participants, leaving us with ten. The participants were requested to have valid driving license. Prior to the start of the experiment, the participants gave their informed consent according to General Motors Institutional Review Board. At the end of the experiment the participants were paid 100 USD.

6.2. Apparatus

Vehicle – the participants were seated in the front passenger seat in order to increase the level of immersion. The participants were able to observe the windshield. The vehicle was driven by a professional driver.
Eye tracking – a system was used to monitor the participants eye movements. The system collected eye gaze locations at 10Hz. RealSense SR300.
GPS – GPS data was collected and aligned with the eye tracking system.

6.3. Design and Procedure

The experiment started when the participant was welcomed and asked to fill a questionnaire. later, the experiment was described and introduced to the participants. The experiment had two driving sessions that shared the same routes. The route was about 10KM long in urban and suburban areas. During the first driving session, the professional driver drove in such a way that imposed relaxed workload on the participant. Later, during the second session, a common workload was imposed. During both sessions, the eye gaze system was activated. In order to keep the participants involved, they were asked to rate the driving.

6.4. Dependent and independent measure

Workload condition – independent measure – Two workload conditions were presented in the experiment: relaxed and common, manipulated by the driver.

Eye gazing distribution – dependent measure – A single eye gaze distribution was estimated during each of the driving sessions. We selected to estimate a single distribution from each ride. Since by doing so we are averaging the diversity of real world environment.

Analysis – reward visualization – The goal of the analysis is to find and observe non-trivial structures and areas in the reward visualization. The VE of the passenger in the front seat, can be divided into two: upper and lower area. Most of the action occurs on the upper area, while in the lower area, almost no activity occurs. More specifically, our goal is to observe the difference between the two areas in the reward visualization. We would like to know, whether we can draw the line between them. For that end, we start by estimating the reward. Let's recall that we estimate the reward only up to some additive and multiplicative constants. The relative relation between the values of the estimated reward are important, much more than the absolute ones. We are using all the eye tracking points that were recorded from all the 10 participants to estimate the matrices P_R and P_C. The following stage is resolution selection. The resolution has to be high enough for visualization of non-trivial areas, and low enough to ensure accurate estimation of bins in a discrete distribution. Finally, we estimate the reward as presented in Eq. 6.

7. RESULTS

Figure 2 presents the results of the experiment. Parts (a) and (b) show the gaze distributions for the relaxed and common conditions respectively. The distributions were estimated using a two-dimensional discrete distribution. Such distribution type was selected to prevent artifacts that are associated with continuous parametric distribution. Although, discrete distribution was selected, the continuous nature of the distribution is easily observed. Both distributions are concentrated around the center and monotonic decay towards the edges of the distribution. The common distribution is less uniform than the relaxed one. The pick of the common distribution is higher than the relaxed pick.

A very different and interesting picture emerges at part (c) – the reward visualization. While the distributions in (a) and (b) concentrated around the center; the reward visualization presents other type of pattern. The visualization suggests two regions: an upper, and lower one. Both regions have a rectangle shape. For better clarity, we drew the broader between them. Each rectangle has its own distinct set of values that differ from the values of the other rectangle. The split between them, resemble the split of the field of view between the upper part of the windshield were most of the action and movement occur, and the lower part, below the windshield, which is mainly dull and constant. Let's recall that our participants are the passengers and have no display in front of them. Another form of visualization is presented at (d). The estimated reward values were split into two group using zero as a threshold. (d) even further demonstrates the existence of two different regions.

Overall, it is important to notice, that two Gaussian-like gazed distribution generated a reward visualization that is very different from Gaussian and semantically meaningful.

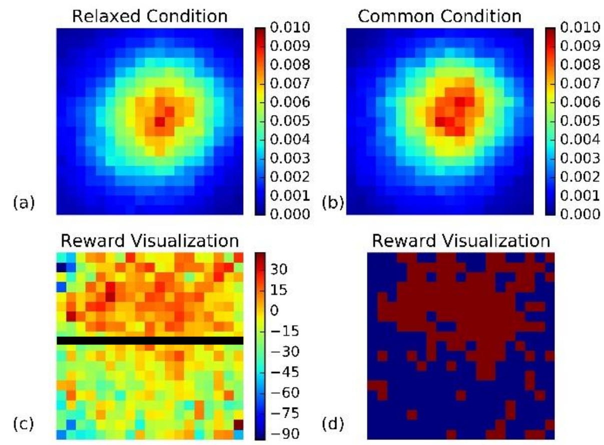

Figure 2. Gaze distribution and reward visualization. (a) and (b) gaze distribution for relaxed and common conditions respectively. (c) reward visualization. (d) quantized reward visualization.

8. CONCLUSION AND DISCUSSION

The results of the experiment show that our suggested visualization mechanism provides non-trivial results that match our expectations. Following those encouraging results, we are considering broadening the usage and evaluation to more complicated tasks and environments. One direction that we would like to pursue is the temporal aspect of the visualization. The limitation of this work is the lack of outside video recordings that prevent us from such pursue.

In addition, those results support the ICC theoretical framework that lead us to the suggested visualization mechanism. ICC [10] [11] has been successfully applied to human model behavior in several contexts before [13] [12] [14], gradually gaining credibility as useful model. We showed its additional capabilities over the STD-based approach [3], and that STD usage can be interpreted as a specific case of ICC. The work presented here has focused on the intuition, mathematical rationale, formulation, and on-road experimental verification of the ICC for reward / important areas visualization, extending the work of [8].

Overall, to put this work at its largest context, we are exploring the flow of information with respect to humans. We are interested in the information they receive from the environment, the information they sent back, and the information they hold. Our work focused mainly on the ICC (as presented here) and the Information Bottleneck (IB) [16].

9. REFERENCES

[1] S. Cox and N. Lavie, "On the efficiency of visual selective attention: Efficient visual search leads to inefficient distractor rejection," *Psychological,* pp. 395-396, 1997.

[2] A. Borji and L. Itti, "State-of-the-art in visual attention modeling," *IEEE Transactions Pattern Analysis and Machine Intelligence,* pp. 185-207, 2013.

[3] T. W. Victor, J. L. Harbluk and J. A. Engstrom, "Sensitivity of eye-movement measures to in-vehicle task difficulty," *Transportation Research Part F: Traffic Psychology and Behaviour,* pp. 167-190, 2005.

[4] L. Itti and P. . F. Baldi, "Bayesian surprise attracts human attention," in *Advances in neural information processing systems*, 2006.

[5] N. Bruce and J. . K. Tsotsos, "Saliency, attention, and visual search: An information theoretic approach," *Journal of vision,* vol. 9.3, 2009.

[6] S. e. a. Hossein Khatoonabadi, "How many bits does it take for a stimulus to be salient?," in *Proceedings of the IEEE Conference on Computer Vision and Pattern Recognition*, 2015.

[7] R. Yashas, P. Le Callet and G. Cheung, "Quantifying the relation between perceived interest and visual salience during free viewing using trellis based optimization," in *Image, Video, and Multidimensional Signal Processing Workshop (IVMSP)*, 2016.

[8] U. Engelke and P. Le Callet, "Perceived interest and overt visual attention in natural images," *Signal Processing: Image Communication,* vol. 39, pp. 386-404, 2015.

[9] . J. Wang, C. Damon and P. Le Callet, "Quantifying the relationship between visual salience and visual importance," *Human Vision and Electronic Imaging,* vol. 7527, 2010.

[10] N. Tishby and D. Polani, "Information theory of decisions and actions," in *Perception-action cycle*, Springer, 2011, pp. 601-636.

[11] J. Rubin, O. Shamir and N. Tishby, "Trading value and information in MDPs," in *Decision Making with Imperfect Decision Makers*, Springer, 2012, pp. 57-74.

[12] R. M. Hecht, A. Bar Hillel, S. Tiomkin, H. Levi, O. Tsimhoni and N. Tishby, "Cognitive workload and vocabulary sparseness: Theory and practice," in *Sixteenth Annual Conference of the International Speech Communication Association*, 2015.

[13] R. M. Hecht, A. Bar Hillel, A. Telpaz, O. Tsimhoni and N. Tishby, "Information constrained control analysis of eye gazing distribution under cognitive workload," *Submitted to IEEE TRANSACTIONS ON HUMAN-MACHINE SYSTEMS.*

[14] R. M. Hecht, A. Telpaz, G. Kamhi, A. Bar Hillel and N. Tishby, "Disentanglement of Top-Down and Bottom-Up Processes Using Information Constrained Control," in *poster without proceedings at the fifth Conference on Cognition Research*, Acre, 2018.

[15] T. M. Cover and J. A. Thomas, "Information Theory and statistics," in *Elements of Information Theory*, 1991.

[16] N. Tishby, F. C. Pereira and W. Bialek, "The information bottleneck method," 2000. [Online]. Available: https://arxiv.org/pdf/physics/0004057.pdf.